COLD SPRING HARBOR
Molecular Case Studies

RESEARCH ARTICLE

Exon skipping in genes encoding lineage-defining myogenic transcription factors in rhabdomyosarcoma

Erin Butler,[1,2,3,6] Lin Xu,[1,2,4,6] Dinesh Rakheja,[2,5] Blake Schwettmann,[1] Shireen Toubbeh,[1] Lei Guo,[4] Jiwoong Kim,[4] Stephen X. Skapek,[1,2,3] and Yanbin Zheng[1,2]

[1]Department of Pediatrics, Division of Hematology/Oncology, University of Texas Southwestern Medical Center, Dallas, Texas 75390, USA; [2]Harold C. Simmons Comprehensive Cancer Center, University of Texas Southwestern Medical Center, Dallas, Texas 75390, USA; [3]Gill Center for Cancer and Blood Disorders, Children's Health Children's Medical Center, Dallas, Texas 75235, USA; [4]Quantitative Biomedical Research Center, Department of Population and Data Sciences, University of Texas Southwestern Medical Center, Dallas, Texas 75390, USA; [5]Department of Pathology, University of Texas Southwestern Medical Center, Dallas, Texas 75390, USA

Abstract Rhabdomyosarcoma (RMS) is a childhood sarcoma composed of myoblast-like cells, which suggests a defect in terminal skeletal muscle differentiation. To explore potential defects in the differentiation program, we searched for mRNA splicing variants in genes encoding transcription factors driving skeletal muscle lineage commitment and differentiation. We studied two RMS cases and identified altered splicing resulting in "skipping" the second of three exons in *MYOD1*. RNA-seq data from 42 tumors and additional RMS cell lines revealed exon 2 skipping in both *MYOD1* and *MYF5* but not in *MYF6* or *MYOG*. Complementary molecular analysis of *MYOD1* mRNA found evidence for exon skipping in five additional RMS cases. Functional studies showed that so-called MYODΔEx2 protein failed to robustly induce muscle-specific genes, and its ectopic expression conferred a selective advantage in cultured fibroblasts and an RMS xenograft. In summary, we present previously unrecognized exon skipping within *MYOD1* and *MYF5* in RMS, and we propose that alternative splicing can represent a mechanism to alter the function of these two transcription factors in RMS.

Corresponding authors: Stephen.Skapek@UTSouthwestern.edu; Yanbin.Zheng@UTSouthwestern.edu

Ontology terms: alveolar rhabdomyosarcoma; embryonal rhabdomyosarcoma

Published by Cold Spring Harbor Laboratory Press

doi:10.1101/mcs.a006190

[Supplemental material is available for this article.]

INTRODUCTION

Rhabdomyosarcoma (RMS), the most common soft tissue sarcoma in children, is distinguished by the expression of genes encoding skeletal muscle regulatory factors (MRFs) and a variety of other structural and functional skeletal muscle proteins (Tonin et al. 1991; Hosoi et al. 1992; Cessna et al. 2001; Sebire and Malone 2003; Saab et al. 2011; Keller and Guttridge 2013). Four major histologic subtypes are recognized: embryonal (ERMS), alveolar (ARMS), spindle cell/sclerosing, and pleomorphic. Most ARMS specimens harbor a balanced chromosomal translocation to generate neomorphic proteins *PAX3–FOXO1* or

[6]These authors contributed equally to this work.

PAX7–FOXO1 and are thus commonly referred to as fusion-positive (FP) RMS. The other fusion-negative forms are often associated with evidence for RAS or receptor tyrosine kinase activation. Light microscopic evidence of poorly differentiated rhabdomyoblasts across the RMS subtypes is consistent with failed terminal differentiation as a common theme in RMS pathogenesis (Tonin et al. 1991; Saab et al. 2011; Keller and Guttridge 2013).

Skeletal muscle lineage commitment and differentiation depends on MRFs, which are basic helix–loop–helix (bHLH) transcription factors encoded by the *MYOD1* family that also includes *MYF5*, *MYOG*, and *MYF6* (Weintraub 1993; Berkes and Tapscott 2005; Saab et al. 2011; Zammit 2017). The molecular basis for their transcriptional activities depends on their capacity to (1) form heterodimers with more widely expressed E proteins encoded by *TCF3*, and (2) bind specific CANNTG enhancer elements, known as E-boxes, in muscle-specific genes (Berkes and Tapscott 2005; Zammit 2017). Additionally, detailed mechanistic studies of mouse MyoD show a requirement for functional RB1 in terminal differentiation in cultured cells and in the mouse (Gu et al. 1993; Novitch et al. 1999; Huh et al. 2004). The RB1 protein facilitates MYOD protein interaction with other transcription factors, including MEF2C (Novitch et al. 1999; Takahashi et al. 2003). The subsequent induction of *Cdkn1a* (Halevy et al. 1995) and *Ink4c* (Franklin and Xiong 1996; Phelps et al. 1998) in differentiating skeletal myocytes enforces an irreversible $G_{0/1}$-phase cell cycle arrest, long-known to coincide with terminal muscle differentiation (Buckingham 1992; Weintraub 1993; Lassar et al. 1994). Although this implies that *MYOD1* should impede RMS formation or progression, some experimental models show that its expression, in fact, confers a selective advantage in RMS (Tenente et al. 2017).

To help explain the seemingly confusing way MYOD may impede or contribute to RMS, we considered how its activity could be regulated. Given the importance of functional RB1 in MYOD activity, it is not surprising that RMS is among the second malignant neoplasms known to occur in children with heritable retinoblastoma and germline *RB1* deficiency (Fabius et al. 2021). Beyond the absence of *RB1*, MYOD activity can be blunted by several mechanisms including blocking MYOD/E protein heterodimer formation by musculin or alternatively spliced *E2A* (Yang et al. 2009); by direct competition of TWIST or SNAIL for MYOD binding to E-boxes (Yang et al. 2009; Soleimani et al. 2012; Skrzypek et al. 2018); or by functional impairment of RB1 by active Cyclin/CDK complexes (Knudsen et al. 1998). MYOD activity can also be derailed by *MYOD1*-intrinsic alterations in RMS. For example, a *MYOD1* point mutation generates $MYOD1^{Leu122Arg}$ in some children and adults with spindle cell/sclerosing RMS (Kohsaka et al. 2014; Agaram et al. 2019). This mutation disrupts a key amino acid (Leu) in the MYOD DNA binding domain (Davis et al. 1990; Weintraub et al. 1991), conferring MYOD with MYC-like properties (Van Antwerp et al. 1992), which drives poor clinical outcomes (Shern et al. 2021).

Propelled by the observation that children and adults with *MYOD1* mutations have dismal clinical outcomes, we considered whether alternative splicing in MRF genes might also represent a mechanism to control their function in RMS. We present two index cases harboring alternative splicing in *MYOD1*. Further bioinformatics studies and functional analyses highlight previously unrecognized "exon skipping" in *MYOD1* and *MYF5* to create a poorly functioning myogenic transcription factor that confers a selective growth advantage when ectopically expressed.

RESULTS

RMS Specimens from Two Children Display Exon 2 Skipping in *MYOD1*

Case #1 Description

A 12-mo-old African American girl presented with infraorbital swelling and redness of the right orbit with concomitant proptosis and rhinorrhea. Magnetic resonance imaging (MRI)

of the brain and orbits showed a T2-enhancing, 8-mm oval mass involving the intra- and extraconal spaces circumscribing the lateral rectus muscle of the right orbit (Fig. 1A, top). The mass extended posteriorly to the orbital apex with resulting displacement and compression of the right optic nerve, but without extension past the orbital fissure. MRI did not reveal any cortical disruption of the orbit, leptomeningeal enhancement, or intracranial abnormalities. Histopathologic examination revealed loose sheets and occasional alveolar arrangements of medium-sized cells with round to ovoid nuclei, vesicular chromatin, small nucleoli, sparse pale cytoplasm, and indistinct cytoplasmic borders; numerous mitotic and apoptotic figures; strong cytoplasmic immunoreactivity for desmin; and 40%–50% nuclear immunoreactivity for myogenin (Fig. 1B, top). Fluorescence in situ hybridization (FISH) was negative for *FOXO1* gene rearrangement. Additional imaging and bone marrow biopsies showed no metastatic disease; hence, the child was determined to have Children's Oncology Group (COG) stage 1, group III disease (Skapek et al. 2019). She was treated as per the COG ARST0331 regimen for low-risk disease. Therapy included 4500-cGy external beam radiation to the primary tumor and systemic chemotherapy including vincristine, dactinomycin, and a cumulative dose of 4.8 g/m^2 of cyclophosphamide (Fig. 1C, top). The child's tumor responded well and the most recent evaluation 9 yr after completing therapy showed no evidence of disease.

Case #2 Description

A 7-yr-old Caucasian female presented to an outside institution with a left-sided, 13 × 5-mm nasal mass, which MRI showed to extend posteriorly to the left medial maxillary sinus (Fig. 1A, bottom). Following a subtotal resection, histopathologic examination of the mass demonstrated a cellular neoplasm with features similar to those described above for Case #1 and immunohistochemical evidence of desmin, myogenin, and MYOD expression. FISH from the outside institution identified *FOXO1* rearrangement, and a final diagnosis of fusion-positive (FP) ARMS was established. Additional imaging and bone marrow biopsy showed no evidence for metastatic disease. In summary, the child was determined to have COG stage 1, group II disease. Given the diagnosis of FP-RMS, she was treated as per the COG ARST0531 study for children with intermediate-risk disease using 3600-cGy external beam radiation to the primary tumor and systemic chemotherapy with vincristine, dactinomycin, and a cumulative dose of 16.8 g/m^2 of cyclophosphamide (Fig. 1C).

Six months following therapy, the child returned to clinic with a left submandibular mass. MRI showed a 2 × 1.5-cm left submandibular lymph node with small nodular recurrence to the primary site in the left maxillary sinus, and a CT chest demonstrated a 4-mm pulmonary nodule. The patient underwent extensive left neck dissection and tumor resection, and the pathology demonstrated lymph node disease with ARMS with anaplastic features (Fig. 1B). The patient received additional systemic chemotherapy using cyclophosphamide and doxorubicin alternating with etoposide and ifosfamide. Disease recurred, though, in the submandibular region ~9 mo later. Additional surgical resection, palliative chemotherapy, and radiation therapy were unsuccessful, and she died of her disease 23 mo from the first relapse (Fig. 1C, bottom).

Molecular Analyses of Clinical Pathology Specimens

RNA was extracted from archival specimens from the Children's Health Children's Medical Center clinical pathology laboratory. Specimens were obtained at diagnosis (case #1) and at first and second relapses (case #2). Total RNA analyzed by semiquantitative RT-PCR followed by ethidium-bromide staining of the fractionated PCR product revealed the presence of forms of *MYOD1* mRNA that included exon 2 and in which exon 2 was "skipped" in all three specimens (Fig. 2A). The "skipped" form of the transcript, which we refer to as

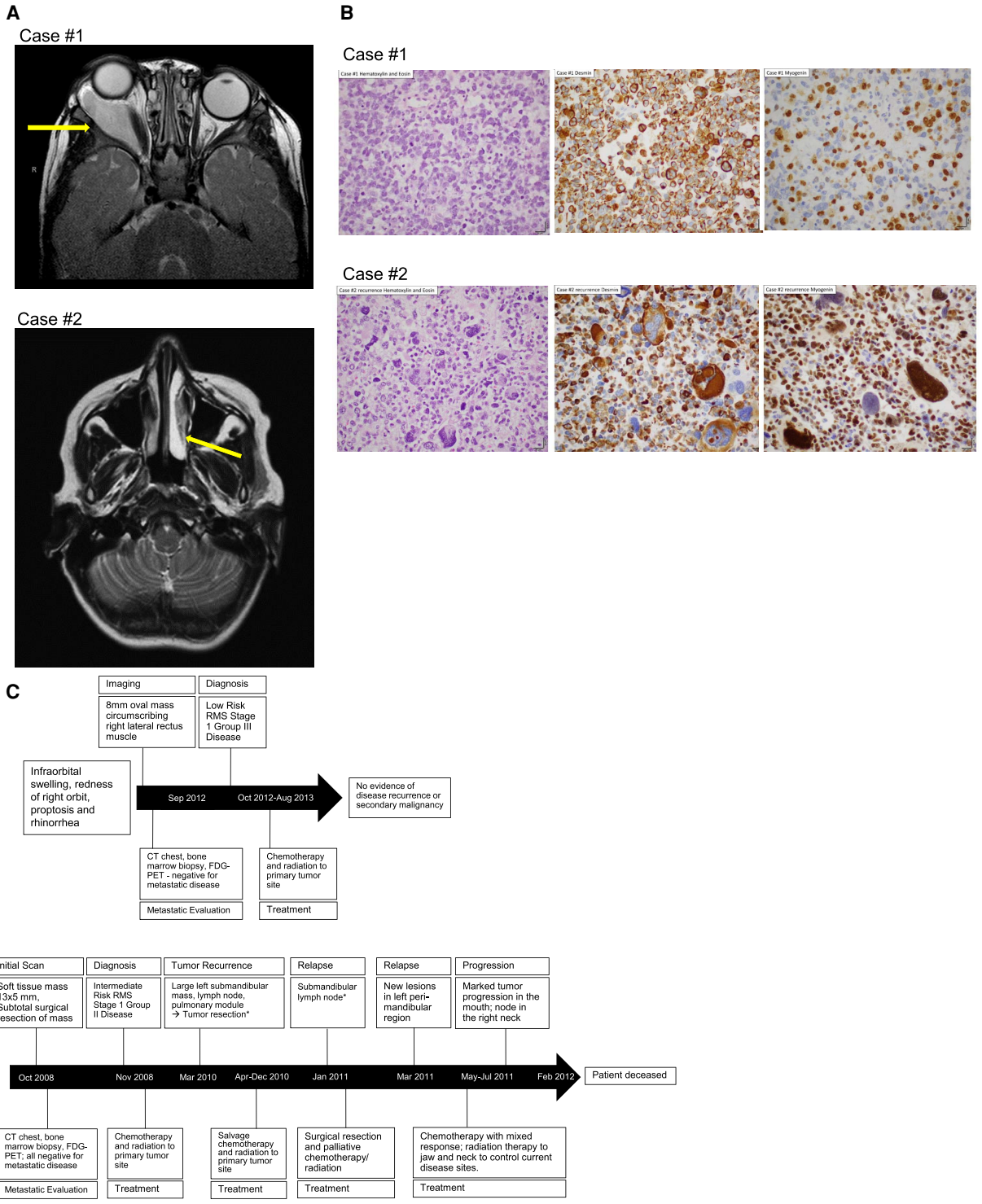

Figure 1. Case presentation of patients with LR-RMS and HR-RMS where *MYOD-ΔEx2* is present. (*A*) MRI at presentation of shows primary orbital tumor and nasal tumors in cases #1 and #2, respectively. Tumors are highlighted by yellow arrows. (*B*) Photomicrographs from cases #1 and #2 showing the typical alveolar rhabomyosarcoma histology and immunoreactivity for desmin and myogenin at diagnosis (case #1) and recurrence (case #2). (*C*) Schematic diagrams display time lines for key events for each of the cases.

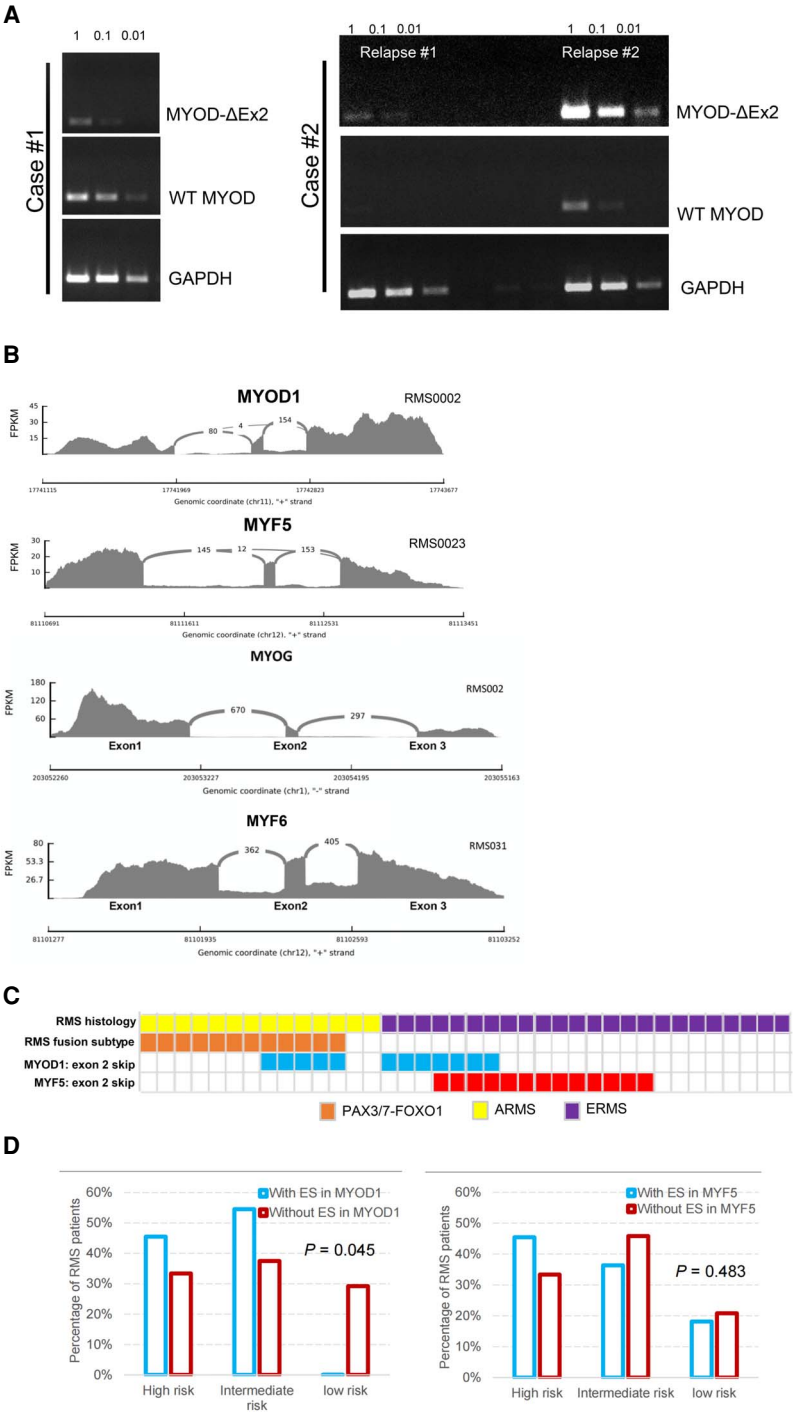

Figure 2. Identifying and confirming *MYOD-ΔEx2* in RMS tumors and cell lines. (*A*) Representative photographs of ethidium bromide-stained agarose gels of the indicated PCR products amplified from serially diluted cDNA generated from case #1 at diagnosis, and from case #2 at first and second relapse. (*B*) Sashimi plots show the read counts spanning the junction of sequential and nonsequential exons of *MYOD1*, *MYF5*, *MYOG*, and *MYF6* in the indicated RMS specimens. (*C*) Schematic diagram displays the distribution of RMS tumors with detectable *MYOD-ΔEx2* and *MYF5-ΔEx2*. The subtype of each tumor (ERMS/ARMS) and the *PAX-FOXO1* fusion status is also displayed. (*D*) Graphs display the percentage of patients with ($n = 11$, blue) or without ($n = 24$, red) evidence for skipping in *MYOD1* or *MYF5* in each of the high-, intermediate-, and low-risk RMS groups.

MYODΔEx2, appeared to be the minor form in all cases. However, the relative level of *MYODΔEx2* versus *MYOD1* seemed higher at the second versus the first relapse in case #2.

Evidence for Exon 2 Skipping in *MYOD1* and *MYF5* Is Commonly Found in RMS

We applied the SplAdder (Kahles et al. 2016) and SpliceFisher algorithms to interrogate more broadly alternative splicing in genes encoding MRFs using published RNA-seq data generated from 42 unique RMS specimens obtained from the St. Jude Data Portal (Chen et al. 2013). We found evidence for exon 2 skipping in either *MYOD1* or *MYF5* in 21 of 42 (50%) RMS specimens (Tables 1, 2; Fig. 2B,C). *MYODΔEx2* and *MYF5ΔEx2* were identified in 12 and 13 cases, respectively, and four cases displayed both. *MYODΔEx2* was relatively equally distributed across fusion-positive (five of 12) and negative (seven of 12) cases, whereas *MYF5ΔEx2*, *MYODΔEx2* expression was expressed in a higher percentage of high and intermediate risk tumors (Fig. 2D). In five RMS-derived cell lines evaluated (RD, RH18, RH30, RH28, and RD-L), we found evidence for exon skipping in three: *MYOD1* (RD-L and RH30) and *MYF5* (RH18) (Supplemental Fig. 1; Supplemental Table 1). In contrast to *MYOD1*

Table 1. Number of supporting reads of MYOD-ΔEx2 transcript and PAX3–FOXO1 fusion transcript in the same sample

	Number of reads spanning junction between exon 1 and exon 2 in MYOD1	Number of reads spanning junction between exon 2 and exon 3 in MYOD1	Number of reads spanning junction between exon 1 and exon 3 in MYOD1	Percent spliced-in (PSI/ψ) scores	PAX3:7–PAX3:8	FOXO1:1–FOXO1:2	PAX3:7–FOXO1:2
RMS001	281	565	11	99.4%	24	56	0
RMS016	155	156	4	98.6%	36	44	0
RMS023	83	94	4	99.4%	37	59	0
RMS047	130	124	6	99.5%	83	40	0
RMS050	206	211	8	99.0%	0	27	0
RMS056	358	407	5	98.7%	1	49	0
RMS057	103	118	3	99.6%	9	42	0
RMS038	197	292	3	98.8%	21	12	5
RMS008	99	134	3	99.3%	10	13	4
RMS036	267	284	4	99.0%	8	13	7
RMS022	739	838	11	99.7%	10	34	15
RMS054	519	534	16	99.4%	10	5	23
RMS002	69	146	0	100.0%	13	12	0
RMS020	116	149	0	100.0%	22	13	0
RMS031	226	220	0	100.0%	53	41	0
RMS039	167	199	0	100.0%	65	58	0
RMS045	291	381	0	100.0%	9	30	0
RMS007	326	362	0	100.0%	5	18	5
RMS044	710	749	0	100.0%	42	31	9
RMS015	205	332	0	100.0%	1	8	11
RMS033	280	264	0	100.0%	59	26	14
RMS035	708	799	0	100.0%	13	3	35

Table 2. Number of supporting reads of MYOG (Myogenin), MYF6, and MYF5ΔEx2 transcripts in the same sample

	Number of reads spanning junction between exon 1 and exon 2 in MYOG	Number of reads spanning junction between exon 2 and exon 3 in MYOG	Number of reads spanning junction between exon 1 and exon 3 in MYOG	Number of reads spanning junction between exon 1 and exon 2 in MYF6	Number of reads spanning junction between exon 2 and exon 3 in MYF6	Number of reads spanning junction between exon 1 and exon 3 in MYF6	Number of reads spanning junction between exon 1 and exon 2 in MYF5	Number of reads spanning junction between exon 2 and exon 3 in MYF5	Number of reads spanning junction between exon 1 and exon 3 in MYF5
RMS001	19	13	0	0	0	0	0	0	0
RMS016	1856	2549	0	6	6	0	592	661	25
RMS023	236	319	0	4	29	0	186	192	13
RMS047	3061	4424	0	19	77	0	574	608	45
RMS050	844	1213	0	0	0	0	328	306	0
RMS056	3254	4514	0	494	697	0	616	618	21
RMS057	2822	4016	0	37	31	0	291	294	0
RMS038	3780	5366	0	0	0	0	26	25	0
RMS008	5262	5605	0	19	18	0	10	8	0
RMS036	4066	5996	0	0	0	0	0	0	0
RMS022	9753	13,905	0	0	0	0	1	0	0
RMS054	11,063	15,737	0	17	11	0	0	0	0
RMS002	379	761	0	206	533	0	573	700	9
RMS020	411	685	0	2	0	0	0	0	0
RMS031	3126	4636	0	380	423	0	542	510	13
RMS039	1508	2088	0	932	1014	0	68	61	0
RMS045	1264	1818	0	0	1	0	0	0	0
RMS007	3934	4434	0	0	0	0	0	0	0
RMS044	6717	8631	0	81	73	0	0	1	0
RMS015	3223	4957	0	2	7	0	5	5	0
RMS033	1660	2502	0	0	0	0	0	0	0
RMS035	7346	9572	0	18	22	0	0	0	0

and *MYF5*, we identified no exon skipping in the other two myogenic bHLH MRFs: *MYOG* and *MYF6* (Table 2; Fig. 2B; Supplemental Table 1). Recognizing that the ability to detect RNA splicing hinges on expression, we note that *MYOG* had the highest average read counts (3706.7 ± 3225.3) and average reads for *MYF6* and *MYF5* were statistically equivalent at 157 ± 270.3 and 290 ± 259.2 ($P = 0.204$), respectively (Table 2).

Using this same data, we also surveyed the exon skipping landscape more globally in RMS, with a specific focus on skipping events found in RMS but not in normal skeletal muscle. Exon skipping was relatively common in skeletal muscle, with more than thirty thousand exons per sample showing evidence of skipping (https://www.gtexportal.org/home/datasets). In our query, we found between 11 and 195 exons per sample that were skipped in RMS but not normal muscle (Supplemental Fig. 2). We plan to report a detailed analysis of those exons elsewhere.

We validated the exon-skipping in *MYOD1* and *MYF5* from RNA-seq using archival RMS specimens and RD-L cells. First, RT-PCR using two different primer pairs confirmed the presence of *MYODΔEx2* in 10 out of 11 archived human RMS specimens with adequate RNA

integrity from our institution (Supplemental Fig. 3A,B). Based on the number of supporting reads from RNA-seq data and semiquantitative analysis of electrophoresed RT-PCR products, the exon-skipped transcript represented a small fraction of total *MYOD1* mRNA in the established tumors and cancer cell lines (Table 1; Fig. 2B). We confirmed the low-level expression by RT-PCR with a single set of primers flanking exon 2 of *MYOD1* and *MYF5* to amplify both forms in one reaction in RMS cells and specimens. Subcloning and sequencing the smaller fragment confirmed the exclusion of exon 2 in cDNA isolated from the RD-L line and RMS sample (Supplemental Fig. 4).

When considering the potential biological significance of low-level expression of an alternatively spliced form of *MYOD1*, we compared the supporting reads of exon-skipped *MYOD1* (three to 16 reads spanning exons 1 and 3) to reads spanning *PAX3* and *FOXO1* to generate the PAX3–FOXO1 fusion oncoprotein (four to 35 reads spanning *PAX3* and *FOXO1*). The average number of reads defining *MYODΔEx2* in the 12 cases where it is detected (6.5 ± 3.99) is similar to the number defining PAX3–FOXO1 in the 10 fusion-positive cases (12.8 ± 9.24; $P = 0.055$) (Table 1). Because a low-level mRNA expression of PAX3–FOXO1 is biologically relevant, similarly low-level expression of *MYODΔEx2* might have a biological effect without acting in a "dominant-negative" fashion.

MYOD1ΔEx2 Fails to Induce Myogenic Differentiation but Does Not Act in a Dominant-Negative Fashion

To explore the functional consequences of exon 2 skipping, we used mouse *MyoD* because expression constructs were available, and the gene structure is conserved between mouse and human with 88% fidelity of amino acids in the orthologous forms (Supplemental Fig. 5). In the mouse and human genes, exon 2 skipping shifts the exon 3 reading frame and truncates the protein. The bHLH domain and the nuclear localization signals are intact, but helix III in the COOH terminus is lost (Fig. 3A,B; Davis et al. 1990; Voronova and Baltimore 1990; Vandromme et al. 1995; Bergstrom and Tapscott 2001).

We engineered MSCV-based retroviral expression vectors to encode either mouse *MyoD1* or *MyoDΔEx2*, linked by an IRES element and cDNA encoding GFP or RFP (Zheng et al. 2013; Iqbal et al. 2016). Transient expression of both forms was detectable in 10T1/2 fibroblasts, but MyoDΔEx2 failed to induce cell elongation or the expression of myogenin or myosin heavy chain, in contrast to wild-type MyoD1 (Fig. 3C,D). Similar findings were observed using the RD cell line, a well-characterized, fusion-negative RMS line (Hiti et al. 1989) that we validated by STR analysis and showed to lack detectable MYOD1 (Fig. 3D; Supplemental Fig. 6; Supplemental Table 2). Consistent with those results, ectopic expression of *MyoD1ΔEx2* only weakly activated the *MCK* enhancer/promoter reporter or a simplified enhancer containing reiterated MYOD-specific E-boxes (Fig. 3E,F), despite its localization to the nucleus in both 10T1/2 and RD cells (Fig. 3H).

Because MYODΔEx2 preserves the bHLH domain that is critical for MYOD1 heterodimerization and DNA binding, we explored whether forced expression of *MYODΔEx2* might exert a dominant-negative action over wild-type MYOD1. As one way to explore this, we transiently coexpressed mouse MyoDΔEx2 with MyoD1 in 10T1/2 fibroblasts and measured the induction of a luciferase reporter driven from the MCK reporter plasmid. In this experimental system, we failed to show a dominant-negative effect (Fig. 3G). Taken together, we conclude that MyoDΔEx2 is a weak inducer of muscle-specific promoters despite retaining DNA-binding and hetero-dimerization motifs and nuclear localization signals, and there is no evidence for a dominant-negative effect when ectopically expressed. We have observed this in cultured fibroblasts and one fusion-negative RMS cell line, but we have not yet studied fusion-positive forms of RMS.

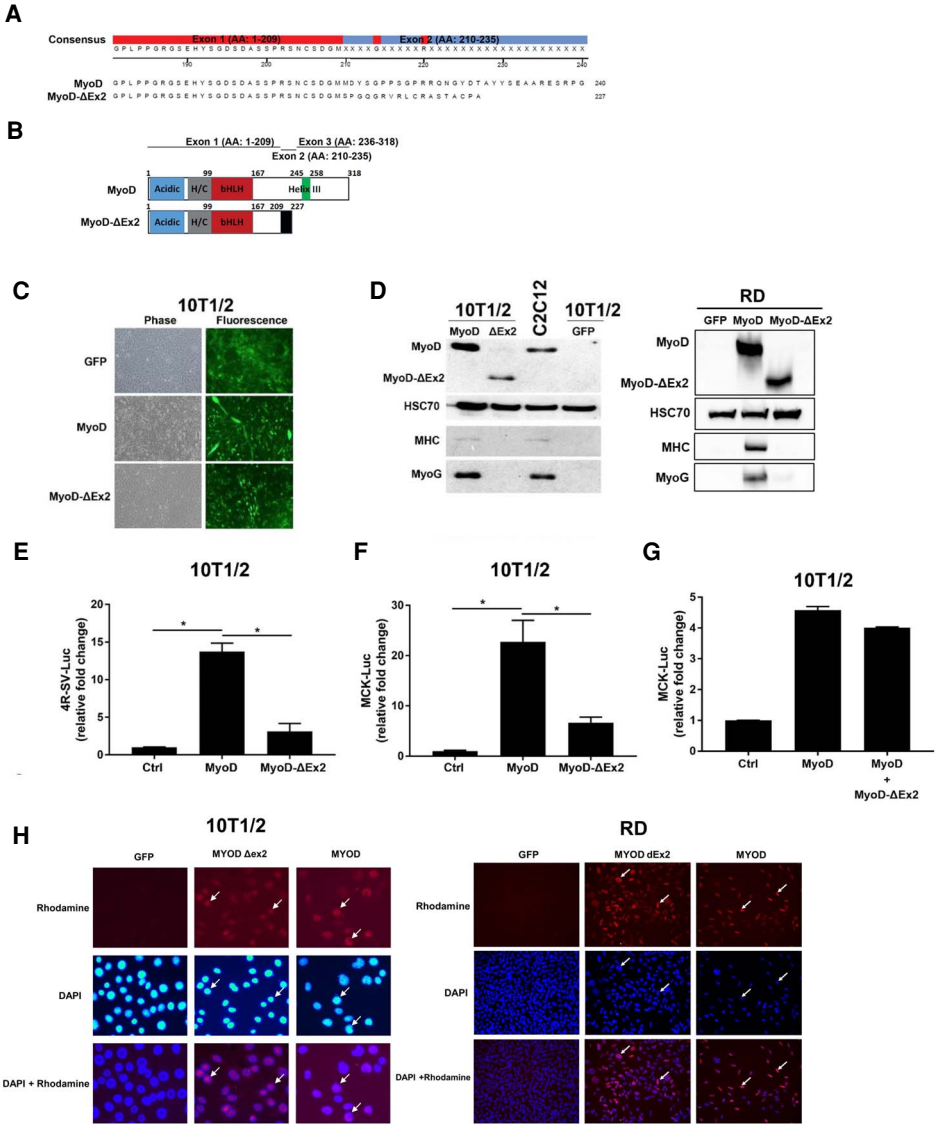

Figure 3. Functional analyses of mouse MyoD-ΔEx2 in 10T1/2 fibroblasts. (*A*) Diagram shows the partial, predicted amino acid sequence of mouse MyoD and MyoD-ΔEx2 spanning the transition between exons 1 and 2 (MyoD) and exons 1 and 3 (MyoD-ΔEx2). Red and blue boxes show similarity and differences, respectively. (*B*) Schematic diagram displays functional motifs of MyoD-ΔEx2 and MyoD proteins, aligned with exons 1, 2, and 3. Note that frame-shift due to exon 2 skipping disrupts Helix III and truncates the protein. (*C*) Representative phase contrast and fluorescence photomicrographs demonstrate that transient expression of MyoD/GFP in 10T1/2 fibroblasts induces cellular elongation not observed in cells transduced with the empty vector (GFP) or the vector encoding MyoD-ΔEx2/GFP. Photos were taken at 40× magnification. (*D*) Representative western blot shows the expression of myosin heavy chain (MHC), myogenin (MyoG), MyoD, and MyoD-ΔEx2 proteins in in the indicated cells after transduction with MyoD- or MyoD-ΔEx2 -expressing retrovirus. C2C12 myoblasts are used as positive control for the western blotting. (*E–G*) Charts demonstrate the induction of luciferase expression when 10T1/2 fibroblasts are transiently transfected with the 4R-SV-Luc (*E*) or MCK-Luc (*F*) reporter plasmids and expression plasmids encoding MyoD, MyoD-ΔEx2, or the empty control vector. Data are displayed as average and standard deviation derived from two different experiments. Asterisks indicate *P*-value <0.05 by two-tailed Student's *t*-test. (*H*) Representative photomicrographs of 10T1/2 fibroblasts and RD cells transduced with retroviral vectors encoding MyoD- or MyoD-ΔEx2 following immunofluorescence staining for MyoD/MyoD-ΔEx2 (rhodamine) or DAPI. Arrows highlight representative, positive cells. Photos were taken at 40× magnification.

Ectopic *MyoD-ΔEx2* Expression Provides a Selective Growth Advantage in Cultured Cells and a Rhabdomyosarcoma Xenograft Model

The continued propagation of cells with functional MYOD1 should be limited because it can enforce cell cycle arrest with differentiation, in essence acting as a tumor suppressor. We established a cell-based model to evaluate this by leveraging retroviral vectors in which MyoD1 expressing cells were marked by GFP and MyoDΔEx2 were marked by RFP. As expected, coculture of 10T1/2 cells stably expressing GFP and RFP showed no enrichment of either population following cultivation and serial passage for 10 d, whereas MyoD(GFP)-expressing fibroblasts were markedly depleted (Fig. 4A). Conversely, coculturing cells expressing either MyoD(GFP) and MyoDΔEx2(RFP) showed enrichment of MyoDΔEx2-expressing cells (Fig. 4B, far right panel). Somewhat surprisingly, MyoDΔEx2-expressing fibroblasts also outcompeted 10T1/2 cells expressing only GFP (Fig. 4B, middle panel). Given the absence of native MyoD1 in 10T1/2 cells, this finding also demonstrates that MyoDΔEx2 is not acting in a dominant-negative fashion with WT MyoD.

We further explored possible dominant-active effects of MyoDΔEx2 by ectopically expressing it in human RD cells. First, in vitro expression of MyoDΔEx2 (RFP) fostered faster cell accumulation than RD cells expressing only RFP (Fig. 4C). Of note, ectopic expression of wild-type MyoD1 in RD cells led to cell elongation and cell arrest similar to that observed in 10T1/2 cells. Second, xenografting transduced RD cells into NOD–SCID mice led to significantly larger tumors 26 d after implantation (Fig. 4D). Third, we noted that MyoDΔEx2 (RFP) expression altered xenograft histology. A representative hematoxylin and eosin-stained section from each of eight xenografts was reviewed by a pediatric pathologist (DR) blinded to their identity. All sections showed spindle and stellate sarcoma cells with scattered large anaplastic cells compatible with ERMS with anaplasia (Fig. 4E). In addition, there were occasional clusters of closely packed cells with round to ovoid nuclei, coarser chromatin, more prominent nucleoli, and high nuclear to cytoplasmic ratio with nuclear molding. While such cells were occasionally seen scattered in the background of all xenografts, clusters of the cells were seen to a variable extent in all four xenografts of MyoDΔEx2 RD cells and in only 1 of 4 RD (RFP) controls (Table 3; Fig. 4E). (Of note, our inability to propagate RD cells ectopically expressing MYOD1 prevented us from using them in this xenograft assay.) In summary, ectopic expression of MyoDΔEx2 can hasten in vitro propagation in fibroblasts and RD cells, increase RD xenograft size, and alter the histology. That MyoDΔEx2 accomplishes this in fibroblasts and RMS cells without detectable *MYOD1* expression further suggests that it can act in a dominant active fashion.

DISCUSSION

Although *MYOD1* and *MYF5* and their roles in skeletal myogenesis have been studied for over 25 yr, little has been published on their potential regulation by alternative splicing, especially in RMS (Skapek et al. 2019). We found evidence for exon-skipping in *MYOD1* in the index cases, and our analysis of additional gene expression data (Chen et al. 2013) revealed low-level exon skipping in *MYOD1* and *MYF5* across a substantial fraction of close to 50 RMS specimens. Functional analyses showed ectopically expressed MyoDΔEx2 localized to the nucleus but only weakly induced skeletal muscle enhancer/promoter reporters and endogenous muscle genes in fibroblasts and an RMS cell line. We note that skipping the second exon shifts the reading frame, so the protein ultimately lacks amino acids encoded by both exons 2 and 3. Interestingly, an early functional study of MyoD1 deletion mutants identified one, DM: 218–269, in which similar amino acids are disrupted (Tapscott et al. 1988). That form displayed decreased capacity to induce myosin in an experimental setting. We found no evidence that MyoDΔEx2 acts in a dominant-negative fashion, even when

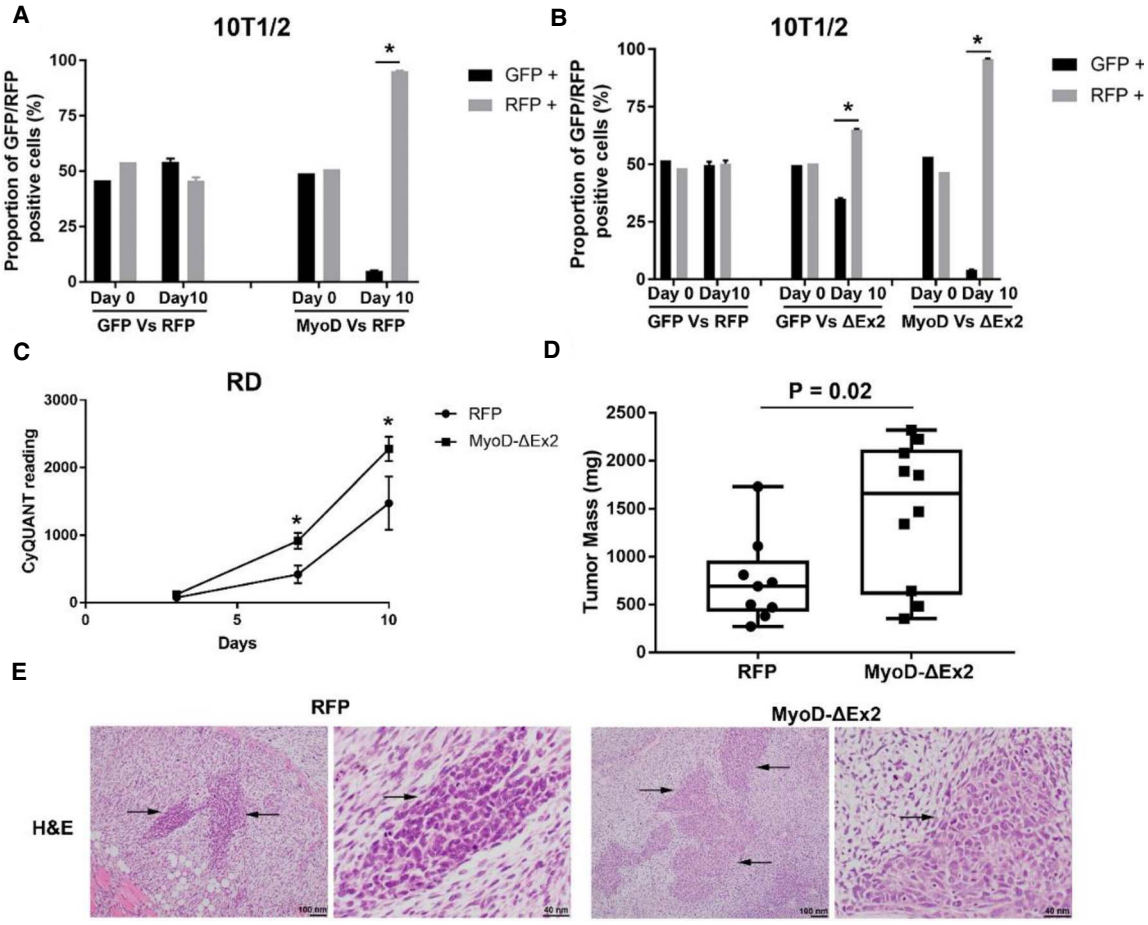

Figure 4. MyoD-ΔEx2 expression provides a growth advantage to 10T1/2 and RD cells. (*A*,*B*) Charts show relative proportion of GFP and RFP-positive in cocultures of 10T1/2 cells transduced with retroviral vectors expressing either MyoD (GFP) or MyoD-ΔEx2 (ΔEx2, RFP) or the empty expression vectors encoding only the GFP or RFP markers. Relative proportion was assessed by flow cytometry on the day of plating (day 0) and after 10 d in growth medium. Quantitative data in *A* and *B*, displayed as average and standard deviation, are derived from three replicates. Asterisks represent *P*-value <0.05 by two-tailed Student's *t*-test. (*C*) Chart displays the number of RD cells following in vitro propagation for the indicated number of days. Cells were transduced with retroviral vectors encoding MyoD-ΔEx2 (RFP) or just RFP and purified by FACS prior to plating. Quantitative data in *C*, displayed as average and standard deviation, are derived from multiple biological replicates ($n = 12$). Asterisks represent *P*-value <0.05 by two-tailed Student's *t*-test. (*D*) Plot displays wet mass of individual xenografts formed by RD cells, transduced and purified as described in *C*, prior to subcutaneous implantation. All tumors were harvested once first experimental tumor reached an average tumor size of 2.0 cm^3. Differences in tumor mass are statistically significant ($P = 0.02$, Mann–Whitney test). (*E*) Representative photomicrographs of hematoxylin and eosin-stained slides of RD xenografts described in *D*. Arrows show representative clusters of closely packed cells.

ectopically expressed. Consistent with an inability to foster differentiation, expressing MyoDΔEx2 boosted cell accumulation over those that expressed wild-type MyoD1. A similar effect in cells with no detectable MYOD1 implied that the altered protein does not act by interfering with full-length MYOD1. In summary, we provide the first evidence for alternative splicing in skeletal muscle lineage transcription factors as a way to generate a protein with altered functional properties in a sarcoma composed of myoblast-like cells.

Table 3. Histologic analysis of RD tumors ectopically expressing MyoD-ΔEx2 or RFP

	Spindles	Stellate	Anaplastic	Clusters of closely packed cells
RFP 280-1	Yes	Yes	Yes	Yes
RFP 280-2	Yes	Yes	Yes	No
RFP 295-4	Yes	Yes	Yes	No
RFP 295-5	Yes	Yes	Yes	No
MyoD-ΔEx2 296-1	Yes	Yes	Yes	Yes
MyoD-ΔEx2 296-3	Yes	Yes	Yes	Yes
MyoD-ΔEx2 296-4	Yes	Yes	Yes	Yes
MyoD-ΔEx2 711-2	Yes	Yes	Yes	Yes

The biological significance of our findings is supported by the lack of evidence for exon skipping in either *MYOG* or *MYF6*. Elegant genetic studies in the mouse previously showed that the four members of this gene family are distinct: *Myod1* and *Myf5* are required for lineage specification, with the accompanying molecular capacity to induce previously silenced muscle gene expression (Braun et al. 1992; Rudnicki et al. 1992, 1993). *Myog* and *Myf6* play roles in later stages of skeletal myogenic differentiation (Hasty et al. 1993; Nabeshima et al. 1993; Zhang et al. 1995). Functional studies of mouse MyoD1 demonstrated that its capacity to induce muscle-specific genes depends on a histidine/cysteine (H/C)-rich motif proximal to the basic-helix-loop-helix motif, and on an amphipathic helix (helix III) toward the carboxyl terminus of the protein (Bergstrom and Tapscott 2001; Berkes et al. 2004). Helix III, present in MyoD1 and Myf5 but not in myogenin (Bergstrom and Tapscott 2001), enables these lineage-defining transcription factors to boost the expression of silenced genes when muscle differentiation begins. The alternative splicing that we describe in *MYOD1* and *MYF5* shifts the reading frame in exon 3 and disrupts helix III. Interestingly, two non-mammalian species—*Ciona intestinalis*, a tunicate species, and *Takifugu rubripes*, a Japanese puffer fish—express a MyoD-like MRF with alternatively spliced forms, one of which lacks helix III (Meedel et al. 1997; Fernandes et al. 2007). Functional studies of the *Ciona* MRF demonstrate that its ectopic expression in the notochord of developing embryos induces muscle genes, and the simultaneous deletion of both H/C and helix III domains significantly reduces its myogenic activity (Izzi et al. 2013). One of the two alternatively spliced forms in *T. rubripes* bypasses exon 2 to disable helix III (Fernandes et al. 2007). One could speculate that developmentally regulated exon 2 skipping in lineage defining MRFs in mammals might also represent a mechanism to dampen the actual initiation of the terminal differentiation process while those cells proliferate or migrate during embryonic development or in skeletal muscle regeneration.

The potential importance of exon skipping in *MYOD1* and *MYF5* merits further exploration in RMS. First, as previously mentioned, a genetic mutation in *MYOD1* that disables its promyogenic effects defines a molecular class of RMS with a uniformly poor prognosis. Our preliminary findings suggest that the presence of *MYOD1* exon skipping may correlate with a higher risk for poor outcome, but that association and whether it is an independent prognostic factor will require further studies using a larger collection of specimens with RNA-seq data and clinical annotation. There are several ways in which exon 2 skipping could directly contribute to RMS formation or progression. First, alternative splicing could represent a novel way to finely tune expression of the full-length, active protein, thereby disabling the capacity to differentiate and cease proliferating. This concept is similar to a previous report showing that alternative splicing of *E2A* (*TCF3*) controls

the level of the DNA binding-competent, heterodimeric partner for MYOD1 (Yang et al. 2009). Second, helix III is required for mouse MyoD1 to interact with Pbx, and that interaction serves as a molecular "beacon" to guide MyoD/E protein heterodimers to the *Myogenin* promoter, essentially initiating differentiation (Berkes et al. 2004). The absence of helix III in the exon skipped form may underlie its weak capacity to enhance muscle gene expression. Finally, it is also possible that an exon-skipped form of MYOD1 (or MYF5) represents a neomorphic protein with the capacity to induce expression of non-muscle genes not typically activated by wild-type forms of those proteins. If so, that could represent a mechanism by which even low-level expression of the exon-skipped transcription factor may influence RMS biology without acting in a dominant-negative fashion. In that regard, it will be interesting to compare the downstream effects of an exon-skipped version of MYOD1 to $MYOD^{Leu122Arg}$, the expression of which now marks a particularly aggressive form of RMS.

METHODS

Cell Lines, Reagents, and RMS Tumors

Cell lines were either provided by P. Houghton (St. Jude Children's Research Hospital) or obtained from ATCC (Saab et al. 2006). 10T1/2 mouse fibroblasts and RMS cell lines RD, RH30, RH18, RH28, RD-L (RD-like; note that RD-L cells have short tandem repeat (STR) features, similar to RD cells) (see Supplemental Table 2), and RH30 were routinely cultivated in DMEM supplemented with 10% FBS, penicillin/streptomycin, and glutamine; C2C12 cells were cultivated in DMEM medium with either 20% FBS (GM) or 2% horse serum with 10 µg/ml insulin (DM + I), with pen/strep and glutamine. Human skeletal muscle myoblasts (HSMM) were purchased from Lonza and maintained in SkGM-2 medium (Lonza). TOPO TA cloning kit was from Thermo Fisher Scientific and used according to the manufacturer's protocol.

RMS patient samples were collected from the University of Texas Southwestern (UTSW) Medical Center and Children's Health Children's Medical Center at Dallas. Collection and analysis of these samples was approved by the UTSW Medical Center Institutional Review Board.

RNA Extraction and RT-PCR

Total RNA was extracted from cells or tumors using the TRIzol reagent (Invitrogen) and cDNA was prepared using SuperScript III RT kits (Invitrogen) as previously described (Zheng et al. 2013). Standard RT-PCR was performed using KAPA HiFi HotStart ReadyMix PCR kit (Kapa Biosystems) according to the manufacturer's protocol. The primers are listed in Tables 4 and 5.

Table 4. Primers for qRT-PCR

Gene	Sense	Antisense
MYOD1	5′-GGCCTTTGAGACACTCAAGC-3′	5′-GATATAGCGGATGGCGTTGC-3′
MYOD1 ΔEx2	5′-CCGACGGCATGAACCCA-3′	5′-AGGGCTCTCGGTGGAGAT-3′
GAPDH	5′-GAAGGTGAAGGTCGGAGTCA-3′	5′-TTGAGGTCAATGAAGGGGTC-3′

Table 5. Primers for PCR

Gene	Sense	Antisense
MYOD1:	5′-CACTACAGCGGCGACTC-3′	5′-AGATGCGCTCCACGATG-3′
mMyod1	5′-CGCAACGCCATCCGCTACAT-3′	5′-ACCTGATAAATCGCATTGGGGTTT-3′

Note that "m" stands for mouse.

MyoD-ΔEx2 Construction, Retrovirus Production, and Infection

CMV-MyoD-ΔEx2 was produced from CMV-Myod1 (Skapek et al. 1995, 1996), which contains wild-type mouse Myod1 cDNA, using QuikChange II XL site-directed mutagenesis kit (Agilent) according to the manufacturer's protocol. Briefly, a PCR reaction was performed using CMV-Myod1 as the template and two complimentary oligonucleotides containing the desired mutation to generate the CMV-M MyoDΔEx2. The PCR primers used for constructing CMV-MyoD-ΔEx2 were: 5′-GCTCTGATGGCATGAGTCCAGGCCAGGG-3′ (sense), 5′-CCCTGGCCTGGACTCATGCCATCAGAGC-3′ (antisense). Then, the template was digested with DpnI and the DpnI-treated DNA product was used to transform XL1-Blue super-competent cells and positive clones were selected. MyoDΔEx2 was confirmed by Sanger sequencing at University of Texas Southwestern Sanger Sequencing Core.

MyoD1 and MyoDΔEx2 cDNA were then excised from CMV-MyoD1 and CMV-MyoD-ΔEx2 by restriction enzyme digestion with EcoRI and subcloned into MSCV-IRES-GFP and/or MSCV-IRES-RFP plasmids (Zheng et al. 2013; Iqbal et al. 2016) at the EcoRI site. Retrovirus was produced by cotransfecting MSCV-based retrovirus vectors with pCAG4-Eco (or pHDM-G), and pMD-Old-Gag-Pol into HEK293 cells. The supernatants were collected at 48 and 72 h, pooled, and filtered with 0.45-μm filter, and aliquots were stored at −80°C for later use.

Reporter Assays

The ability of MyoD1 and MyoDΔEx2 to induce muscle specific promoters was assessed by cotransfecting 10T1/2 fibroblasts using these expression plasmids and luciferase reporters: p3300 MCK-Luc or p4R-SV-Luc, as previously described (Wilson et al. 2016). The p3300 MCK-Luc contains 3300 bp from the muscle creatine kinase (MCK) promoter and p4R-SV-Luc contains four MyoD-binding E-boxes and a minimal SV40 promoter, analogous to previously described plasmids containing the chloramphenicol acetyl transferase (CAT) reporter (Skapek et al. 1995, 1996). Firefly luciferase, normalized to *Renilla* luciferase, was measured as previously described (Wilson et al. 2016).

Protein Expression

Western blotting was performed as previously described (Zheng et al. 2010) using antibodies against HSC70 (loading control; catalog # 7298) and MyoD (catalog # 760) (both from Santa Cruz Biotechnology, Inc); myogenin (BD Pharmingen catalog # 556358), and MHC (Millipore catalog # 05-716).

Immunofluorescence Staining for MyoD/MyoD-dEx2

RD and 10T1/2 cells transduced with GFP, MyoD-, or MyoDΔEx2-encoding retroviral vectors were rinsed with PBS and fixed in 1 mL of 4% PFA for 10 min at room temperature. They were then washed with PBS and permeabilized with 0.1% Triton X-100 for 10 min. Cells then incubated in 4% goat serum for 1 h before adding MYOD1 primary antibody (1:50 dilution in 4% goat serum; Invitrogen # MA5-12902). They were incubated overnight at 4°C while

shaking. The cells were then washed with PBS before incubating with rhodamine anti-mouse secondary antibody (1:200 dilution in 4% goat serum; Abcam # ab9093) for 1 h at room temperature. Finally, cells were washed with PBS and incubated with DAPI (1:1000 dilution) and imaged with fluorescence using the Lumenera INFINITY3-6UR microscopy camera at 40× magnification.

Coculture Experiments

10T1/2 cells transduced with either retrovirus containing *MyoDΔEx2* (RFP), *Myod1* (GFP), or encoding GFP or RFP alone and cocultured. Flow cytometry was performed at the beginning of each coculture experiment to ensure a 1:1 ratio of green and red fluorescent cells. The mixed cells were cultivated in triplicate wells and passaged at a 1:10 ratio every 3 d for a total of 10 d, at which time they were again analyzed by flow cytometry. The relative number of each cell population was calculated and presented as a fraction of the total fluorescently labeled cells.

Cell Accumulation Assays and Xenografts

Cell accumulation was measured in vitro using CyQUANT cell proliferation assay kit (Thermo Fisher Scientific) according to the manufacturers' instructions. Cells (1×10^3) were seeded in each well of 96-well plates with six replicates and harvested following 10 d. The data were plotted with readings of CyQUANT assay from different time points.

For in vivo tumorigenesis assay, 5×10^6 RD cells transduced with either *RFP* or *MyoDΔEx2–RFP* vectors were resuspended in PBS and Matrigel (1:1 ratio) and injected subcutaneously in bilateral flanks of NOD/SCID mice purchased from UTSW breeding core (8–12 wk old, 10 animals/group). Tumor size was measured two to three times weekly by calipers and volume was calculated as follows: volume = $[(\text{width})^2 \times \text{length}]/2$ where width was the smallest of two measurements obtained. Endpoint tumor size was adopted at 2.0 cm^3, and mice bearing *RFP* or *MyoDΔEx2-RFP* tumors were euthanized by CO_2 at the same time. Tumors were harvested and processed for routine histology and immunohistochemical analyses as previously described (Zheng et al. 2013). All research involving animals was conducted according to protocols approved by the UT SW Medical Center Institutional Animal Care and Use Committee (IACUC).

Bioinformatics Analyses

We applied for RNA-seq data of 42 RMS specimens from the St. Jude data portal (https://platform.stjude.cloud/) and downloaded the FASTQ files after obtaining permission. The SplAdder algorithm (Kahles et al. 2016) was used to extract all RNA-seq reads spanning splicing junction of any two exons within the same gene. In other words, only reads that can align partially with one exon and also align the rest of part with another exon were maintained and further examined. The original source code of SplAdder is available at https://github.com/ratschlab/spladder. Another independent approach, SpliceFisher algorithm (https://github.com/jiwoongbio/SpliceFisher), was used to validate all exon-skipping events identified by SplAdder algorithm. We first set an Anaconda (version 2.4.1 [64-bit], https://www.anaconda.com/) environment to organize dependencies, and then installed NumPy (version 1.15.0), Matplotlib (version 1.5.2), SciPy (version 0.16.1), intervaltree (version 3.0.0), H5py (version 2.3), Pysam (version 0.10.0), statsmodels (version 0.9.0), and SplAdder directly from source code (https://github.com/ratschlab/spladder) under Python (version 3.4.3). After setting up the environment, we then ran SplAdder command lines with default parameter settings recommended by the SplAdder team (https://github.com/ratschlab/spladder/wiki). Exon information was downloaded from Gencode database (https://www.gencodegenes.org/) based on version 24. Compared with all defined consecutive exons from Gencode annotation, SplAdder further extracted all reads spanning non-consecutive

exons, which are reads supporting exon-skipping events. As suggested by previous publications (Zhang et al. 2016; Vu et al. 2018), we requested at least three supporting reads spanning non-consecutive exons to define an exon-skipping event. Applying SplAdder algorithm to RNA-seq data from 42 RMS tumors downloaded from the European Genome–phenome Archive (EGA) with accession number EGAD00001000878, we identified exon 2-skipping alterations in *MYOD1* gene and *MYF5* gene, separately. These findings were confirmed by SpliceFisher algorithm. RNA-seq data for additional tumors are from TCGA, which was downloaded from GDC portal (https://portal.gdc.cancer.gov/). The normal tissue RNA-seq data was downloaded from GTEX portal (https://gtexportal.org/home/datasets).

Statistical Analysis

Quantitative data are presented as a mean with standard deviation from three or more representative experiments. Statistical significance (P-value <0.05) was calculated using the unpaired Student's t-test.

ADDITIONAL INFORMATION

Data Deposition and Access

The data supporting the findings of this study are available within the article and its Supplemental Information files. RNA-seq data generated from this study are publicly available at NCBI Gene Expression Omnibus with accession number of GSE210475.

Ethics Statement

Patients consented to research and tissue collection under IRB STU 082010-115; phenotypic and tissue analyzation conducted under IRB STU 102011-034.

Acknowledgments

We gratefully acknowledge J. Liu, M. Hassan, and P. Liem for technical assistance, and all other Skapek laboratory members for helpful discussions.

Author Contributions

L.X., S.X.S., and Y.Z. conceived the study. E.B., L.X., J.K., and L.G. ran the software and performed the bioinformatics and statistical analysis. Investigation, E.B., D.R., B.S., S.T., and Y.Z. performed the investigation. E.B., L.X., S.X.S., and Y.Z. wrote the original draft of the manuscript. E.B., L.X., D.R., J.K., S.T., B.S., S.X.S., and Y.Z. reviewed and edited the manuscript. S.X.S. supervised the study. E.B., L.X., S.X.S., and Y.Z. acquired the funding.

Funding

This research is partially supported by grants to E.B. from the 5 K12 HD 68369-10 K12 Scholar Award, Children's Cancer Fund (Dallas), and Hyundai Hope on Wheels Foundation; to L.X. from the Rally Foundation and Children's Cancer Fund (Dallas), as well as computational resource support from Texas Advanced Computing Center (TACC); to S.X.S. from the Cancer Prevention and Research Institute of Texas (RP180319) and University of Texas Southwestern Harold C. Simmons Comprehensive Cancer Center from the National Cancer Institute (CA142543); and to Y.Z. from the Hyundai Hope on Wheels Foundation, Andrew McDonough B+ Foundation, and Children's Cancer Fund (Dallas).

Competing Interest Statement

The authors have declared no competing interest.

Received January 5, 2022; accepted in revised form July 25, 2022.

REFERENCES

Agaram NP, LaQuaglia MP, Alaggio R, Zhang L, Fujisawa Y, Ladanyi M, Wexler LH, Antonescu CR. 2019. MYOD1-mutant spindle cell and sclerosing rhabdomyosarcoma: an aggressive subtype irrespective of age. A reappraisal for molecular classification and risk stratification. *Mod Pathol* **32:** 27–36. doi:10.1038/s41379-018-0120-9

Bergstrom DA, Tapscott SJ. 2001. Molecular distinction between specification and differentiation in the myogenic basic helix–loop–helix transcription factor family. *Mol Cell Biol* **21:** 2404–2412. doi:10.1128/MCB.21.7.2404-2412.2001

Berkes CA, Tapscott SJ. 2005. MyoD and the transcriptional control of myogenesis. *Semin Cell Dev Biol* **16:** 585–595. doi:10.1016/j.semcdb.2005.07.006

Berkes CA, Bergstrom DA, Penn BH, Seaver KJ, Knoepfler PS, Tapscott SJ. 2004. Pbx marks genes for activation by MyoD indicating a role for a homeodomain protein in establishing myogenic potential. *Mol Cell* **14:** 465–477. doi:10.1016/S1097-2765(04)00260-6

Braun T, Rudnicki MA, Arnold HH, Jaenisch R. 1992. Targeted inactivation of the muscle regulatory gene *Myf-5* results in abnormal rib development and perinatal death. *Cell* **71:** 369–382. doi:10.1016/0092-8674(92)90507-9

Buckingham M. 1992. Making muscle in mammals. *Trends Genet* **8:** 144–148. doi:10.1016/0168-9525(92)90081-E

Cessna MH, Zhou H, Perkins SL, Tripp SR, Layfield L, Daines C, Coffin CM. 2001. Are myogenin and myoD1 expression specific for rhabdomyosarcoma? A study of 150 cases, with emphasis on spindle cell mimics. *Am J Surg Pathol* **25:** 1150–1157. doi:10.1097/00000478-200109000-00005

Chen X, Stewart E, Shelat AA, Qu C, Bahrami A, Hatley M, Wu G, Bradley C, McEvoy J, Pappo A, et al. 2013. Targeting oxidative stress in embryonal rhabdomyosarcoma. *Cancer Cell* **24:** 710–724. doi:10.1016/j.ccr.2013.11.002

Davis RL, Cheng PF, Lassar AB, Weintraub H. 1990. The MyoD DNA binding domain contains a recognition code for muscle-specific gene activation. *Cell* **60:** 733–746. doi:10.1016/0092-8674(90)90088-V

Fabius AWM, van Hoefen Wijsard M, van Leeuwen FE, Moll AC. 2021. Subsequent malignant neoplasms in retinoblastoma survivors. *Cancers (Basel)* **13:** 1200. doi:10.3390/cancers13061200

Fernandes JM, Kinghorn JR, Johnston IA. 2007. Differential regulation of multiple alternatively spliced transcripts of *MyoD*. *Gene* **391:** 178–185. doi:10.1016/j.gene.2006.12.015

Franklin DS, Xiong Y. 1996. Induction of p18INK4c and its predominant association with CDK4 and CDK6 during myogenic differentiation. *Mol Biol Cell* **7:** 1587–1599. doi:10.1091/mbc.7.10.1587

Gu W, Schneider JW, Condorelli G, Kaushal S, Mahdavi V, Nadal-Ginard B. 1993. Interaction of myogenic factors and the retinoblastoma protein mediates muscle cell commitment and differentiation. *Cell* **72:** 309–324. doi:10.1016/0092-8674(93)90110-C

Halevy O, Novitch BG, Spicer DB, Skapek SX, Rhee J, Hannon GJ, Beach D, Lassar AB. 1995. Correlation of terminal cell cycle arrest of skeletal muscle with induction of p21 by MyoD. *Science* **267:** 1018–1021. doi:10.1126/science.7863327

Hasty P, Bradley A, Morris JH, Edmondson DG, Venuti JM, Olson EN, Klein WH. 1993. Muscle deficiency and neonatal death in mice with a targeted mutation in the myogenin gene. *Nature* **364:** 501–506. doi:10.1038/364501a0

Hiti AL, Bogenmann E, Gonzales F, Jones PA. 1989. Expression of the MyoD1 muscle determination gene defines differentiation capability but not tumorigenicity of human rhabdomyosarcomas. *Mol Cell Biol* **9:** 4722–4730. doi:10.1128/mcb.9.11.4722-4730.1989

Hosoi H, Sugimoto T, Hayashi Y, Inaba T, Horii Y, Morioka H, Fushiki S, Hamazaki M, Sawada T. 1992. Differential expression of myogenic regulatory genes, MyoD1 and myogenin, in human rhabdomyosarcoma sublines. *Int J Cancer* **50:** 977–983. doi:10.1002/ijc.2910500626

Huh MS, Parker MH, Scimè A, Parks R, Rudnicki MA. 2004. Rb is required for progression through myogenic differentiation but not maintenance of terminal differentiation. *J Cell Biol* **166:** 865–876. doi:10.1083/jcb.200403004

Iqbal NS, Devitt CC, Sung CY, Skapek SX. 2016. $p19^{Arf}$ limits primary vitreous cell proliferation driven by PDGF-B. *Exp Eye Res* **145:** 224–229. doi:10.1016/j.exer.2016.01.004

Izzi SA, Colantuono BJ, Sullivan K, Khare P, Meedel TH. 2013. Functional studies of the *Ciona intestinalis* myogenic regulatory factor reveal conserved features of chordate myogenesis. *Dev. Biol* **376:** 213–223. doi:10.1016/j.ydbio.2013.01.033

Kahles A, Ong CS, Zhong Y, Ratsch G. 2016. Spladder: identification, quantification and testing of alternative splicing events from RNA-seq data. *Bioinformatics* **32:** 1840–1847. doi:10.1093/bioinformatics/btw076

Keller C, Guttridge DC. 2013. Mechanisms of impaired differentiation in rhabdomyosarcoma. *FEBS J* **280:** 4323–4334. doi:10.1111/febs.12421

Knudsen ES, Pazzagli C, Born TL, Bertolaet BL, Knudsen KE, Arden KC, Henry RR, Feramisco JR. 1998. Elevated cyclins and cyclin-dependent kinase activity in the rhabdomyosarcoma cell line RD. *Cancer Res* **58:** 2042–2049.

Kohsaka S, Shukla N, Ameur N, Ito T, Ng CK, Wang L, Lim D, Marchetti A, Viale A, Pirun M, et al. 2014. A recurrent neomorphic mutation in *MYOD1* defines a clinically aggressive subset of embryonal rhabdomyosarcoma associated with PI3K–AKT pathway mutations. *Nat Genet* **46:** 595–600. doi:10.1038/ng.2969

Lassar AB, Skapek SX, Novitch B. 1994. Regulatory mechanisms that coordinate skeletal muscle differentiation and cell cycle withdrawal. *Curr Opin Cell Biol* **6:** 788–794. doi:10.1016/0955-0674(94)90046-9

Meedel TH, Farmer SC, Lee JJ. 1997. The single MyoD family gene of *Ciona intestinalis* encodes two differentially expressed proteins: implications for the evolution of chordate muscle gene regulation. *Development* **124:** 1711–1721. doi:10.1242/dev.124.9.1711

Nabeshima Y, Hanaoka K, Hayasaka M, Esumi E, Li S, Nonaka I, Nabeshima Y. 1993. Myogenin gene disruption results in perinatal lethality because of severe muscle defect. *Nature* **364:** 532–535. doi:10.1038/364532a0

Novitch BG, Spicer DB, Kim PS, Cheung WL, Lassar AB. 1999. pRb is required for MEF2-dependent gene expression as well as cell-cycle arrest during skeletal muscle differentiation. *Curr Biol* **9:** 449–459. doi:10.1016/S0960-9822(99)80210-3

Phelps DE, Hsiao KM, Li Y, Hu N, Franklin DS, Westphal E, Lee EY, Xiong Y. 1998. Coupled transcriptional and translational control of cyclin-dependent kinase inhibitor $p18^{INK4c}$ expression during myogenesis. *Mol Cell Biol* **18:** 2334–2343. doi:10.1128/MCB.18.4.2334

Rudnicki MA, Braun T, Hinuma S, Jaenisch R. 1992. Inactivation of *MyoD* in mice leads to up-regulation of the myogenic HLH gene *Myf-5* and results in apparently normal muscle development. *Cell* **71:** 383–390. doi:10.1016/0092-8674(92)90508-A

Rudnicki MA, Schnegelsberg PN, Stead RH, Braun T, Arnold HH, Jaenisch R. 1993. MyoD or Myf-5 is required for the formation of skeletal muscle. *Cell* **75:** 1351–1359. doi:10.1016/0092-8674(93)90621-V

Saab R, Bills JL, Miceli AP, Anderson CM, Khoury JD, Fry DW, Navid F, Houghton PJ, Skapek SX. 2006. Pharmacologic inhibition of cyclin-dependent kinase 4/6 activity arrests proliferation in myoblasts and rhabdomyosarcoma-derived cells. *Mol Cancer Ther* **5:** 1299–1308. doi:10.1158/1535-7163.MCT-05-0383

Saab R, Spunt SL, Skapek SX. 2011. Myogenesis and rhabdomyosarcoma the Jekyll and Hyde of skeletal muscle. *Curr Top Dev Biol* **94:** 197–234. doi:10.1016/B978-0-12-380916-2.00007-3

Sebire NJ, Malone M. 2003. Myogenin and MyoD1 expression in paediatric rhabdomyosarcomas. *J Clin Pathol* **56:** 412–416. doi:10.1136/jcp.56.6.412

Shern JF, Selfe J, Izquierdo E, Patidar R, Chou HC, Song YK, Yohe ME, Sindiri S, Wei J, Wen X, et al. 2021. Genomic classification and clinical outcome in rhabdomyosarcoma: a report from an international consortium. *J Clin Oncol* **39:** 2859–2871. doi:10.1200/JCO.20.03060

Skapek SX, Rhee J, Spicer DB, Lassar AB. 1995. Inhibition of myogenic differentiation in proliferating myoblasts by cyclin D1-dependent kinase. *Science* **267:** 1022–1024. doi:10.1126/science.7863328

Skapek SX, Rhee J, Kim PS, Novitch BG, Lassar AB. 1996. Cyclin-mediated inhibition of muscle gene expression via a mechanism that is independent of pRB hyperphosphorylation. *Mol Cell Biol* **16:** 7043–7053. doi:10.1128/MCB.16.12.7043

Skapek SX, Ferrari A, Gupta AA, Lupo PJ, Butler E, Shipley J, Barr FG, Hawkins DS. 2019. Rhabdomyosarcoma. *Nat Rev Dis Primers* **5:** 1. doi: 10.1038/s41572-018-0051-2

Skrzypek K, Kusienicka A, Trzyna E, Szewczyk B, Ulman A, Konieczny P, Adamus T, Badyra B, Kortylewski M, Majka M. 2018. SNAIL is a key regulator of alveolar rhabdomyosarcoma tumor growth and differentiation through repression of MYF5 and MYOD function. *Cell Death Dis* **9:** 643. doi: 10.1038/s41419-018-0693-8

Soleimani VD, Yin H, Jahani-Asl A, Ming H, Kockx CE, van Ijcken WF, Grosveld F, Rudnicki MA. 2012. Snail regulates MyoD binding-site occupancy to direct enhancer switching and differentiation-specific transcription in myogenesis. *Mol Cell* **47:** 457–468. doi:10.1016/j.molcel.2012.05.046

Takahashi C, Bronson RT, Socolovsky M, Contreras B, Lee KY, Jacks T, Noda M, Kucherlapati R, Ewen ME. 2003. *Rb* and N-*ras* function together to control differentiation in the mouse. *Mol Cell Biol* **23:** 5256–5268. doi:10.1128/MCB.23.15.5256-5268.2003

Tapscott SJ, Davis RL, Thayer MJ, Cheng PF, Weintraub H, Lassar AB. 1988. MyoD1: a nuclear phosphoprotein requiring a Myc homology region to convert fibroblasts to myoblasts. *Science* **242:** 405–411. doi:10.1126/science.3175662

Tenente IM, Hayes MN, Ignatius MS, McCarthy K, Yohe M, Sindiri S, Gryder B, Oliveira ML, Ramakrishnan A, Tang Q, et al. 2017. Myogenic regulatory transcription factors regulate growth in rhabdomyosarcoma. *Elife* **6:** e19214. doi:10.7554/eLife.19214

Tonin PN, Scrable H, Shimada H, Cavenee WK. 1991. Muscle-specific gene expression in rhabdomyosarcomas and stages of human fetal skeletal muscle development. *Cancer Res* **51:** 5100–5106.

Van Antwerp ME, Chen DG, Chang C, Prochownik EV. 1992. A point mutation in the MyoD basic domain imparts c-Myc-like properties. *Proc Natl Acad Sci* **89:** 9010–9014. doi:10.1073/pnas.89.19.9010

Vandromme M, Cavadore JC, Bonnieu A, Froeschle A, Lamb N, Fernandez A. 1995. Two nuclear localization signals present in the basic-helix 1 domains of MyoD promote its active nuclear translocation and can function independently. *Proc Natl Acad Sci* **92:** 4646–4650. doi:10.1073/pnas.92.10.4646

Voronova A, Baltimore D. 1990. Mutations that disrupt DNA binding and dimer formation in the E47 helix–loop–helix protein map to distinct domains. *Proc Natl Acad Sci* **87:** 4722–4726. doi:10.1073/pnas.87.12.4722

Vu TN, Deng W, Trac QT, Calza S, Hwang W, Pawitan Y. 2018. A fast detection of fusion genes from paired-end RNA-seq data. *BMC Genomics* **19:** 786. doi:10.1186/s12864-018-5156-1

Weintraub H. 1993. The MyoD family and myogenesis: redundancy, networks, and thresholds. *Cell* **75:** 1241–1244. doi:10.1016/0092-8674(93)90610-3

Weintraub H, Dwarki VJ, Verma I, Davis R, Hollenberg S, Snider L, Lassar A, Tapscott SJ. 1991. Muscle-specific transcriptional activation by MyoD. *Genes Dev* **5:** 1377–1386. doi:10.1101/gad.5.8.1377

Wilson RA, Liu J, Xu L, Annis J, Helmig S, Moore G, Timmerman C, Grandori C, Zheng Y, Skapek SX. 2016. Negative regulation of initial steps in skeletal myogenesis by mTOR and other kinases. *Sci Rep* **6:** 20376. doi:10.1038/srep20376

Yang Z, MacQuarrie KL, Analau E, Tyler AE, Dilworth FJ, Cao Y, Diede SJ, Tapscott SJ. 2009. MyoD and E-protein heterodimers switch rhabdomyosarcoma cells from an arrested myoblast phase to a differentiated state. *Genes Dev* **23:** 694–707. doi:10.1101/gad.1765109

Zammit PS. 2017. Function of the myogenic regulatory factors Myf5, MyoD, Myogenin and MRF4 in skeletal muscle, satellite cells and regenerative myogenesis. *Semin Cell Dev Biol* **72:** 19–32. doi:10.1016/j.semcdb.2017.11.011

Zhang W, Behringer RR, Olson EN. 1995. Inactivation of the myogenic bHLH gene *MRF4* results in up-regulation of myogenin and rib anomalies. *Genes Dev* **9:** 1388–1399. doi:10.1101/gad.9.11.1388

Zhang J, White NM, Schmidt HK, Fulton RS, Tomlinson C, Warren WC, Wilson RK, Maher CA. 2016. Integrate: gene fusion discovery using whole genome and transcriptome data. *Genome Res* **26:** 108–118. doi:10.1101/gr.186114.114

Zheng Y, Zhao YD, Gibbons M, Abramova T, Chu PY, Ash JD, Cunningham JM, Skapek SX. 2010. Tgfβ signaling directly induces *Arf* promoter remodeling by a mechanism involving Smads 2/3 and p38 MAPK. *J Biol Chem* **285:** 35654–35664. doi:10.1074/jbc.M110.128959

Zheng Y, Devitt C, Liu J, Mei J, Skapek SX. 2013. A distant, *cis*-acting enhancer drives induction of *Arf* by Tgfβ in the developing eye. *Dev Biol* **380:** 49–57. doi:10.1016/j.ydbio.2013.05.003